Neurobiology of Disease

The *ataxia3* Mutation in the N-Terminal Cytoplasmic Domain of Sodium Channel $Na_v1.6$ Disrupts Intracellular Trafficking

Lisa M. Sharkey,[1] Xiaoyang Cheng,[2] Valerie Drews,[1] David A. Buchner,[1] Julie M. Jones,[1] Monica J. Justice,[3] Stephen G. Waxman,[2] Sulayman D. Dib-Hajj,[2]* and Miriam H. Meisler[1]*

[1]Department of Human Genetics, University of Michigan, Ann Arbor, Michigan 48109-5618, [2]Department of Neurology, Yale University, New Haven, Connecticut 06520-8018, and [3]Departments of Molecular and Human Genetics and Molecular Physiology and Biophysics, Baylor College of Medicine, Houston, Texas 77030

The ENU-induced neurological mutant *ataxia3* was mapped to distal mouse chromosome 15. Sequencing of the positional candidate gene *Scn8a* encoding the sodium channel $Na_v1.6$ identified a T>C transition in exon 1 resulting in the amino acid substitution p.S21P near the N terminus of the channel. The cytoplasmic N-terminal region is evolutionarily conserved but its function has not been well characterized. *ataxia3* homozygotes exhibit a severe disorder that includes ataxia, tremor, and juvenile lethality. Unlike *Scn8a* null mice, they retain partial hindlimb function. The mutant transcript is stable but protein abundance is reduced and the mutant channel is not detected in its usual site of concentration at nodes of Ranvier. In whole-cell patch-clamp studies of transfected ND7/23 cells that were maintained at 37°C, the mutant channel did not produce sodium current, and function was not restored by coexpression of $\beta1$ and $\beta2$ subunits. However, when transfected cells were maintained at 30°C, the mutant channel generated voltage-dependent inward sodium currents with an average peak current density comparable with wild type, demonstrating recovery of channel activity. Immunohistochemistry of primary cerebellar granule cells from *ataxia3* mice demonstrated that the mutant protein is retained in the *cis*-Golgi. This trafficking defect can account for the low level of $Na_v1.6$-S21P at nodes of Ranvier *in vivo* and at the surface of transfected cells. The data demonstrate that the cytoplasmic N-terminal domain of the sodium channel is required for anterograde transport from the Golgi complex to the plasma membrane.

Introduction

Scn8a encodes the sodium channel $Na_v1.6$, which is expressed in neurons of the CNS and PNS. In addition to its localization on cell bodies, dendrites, and unmyelinated axons, $Na_v1.6$ is the predominant sodium channel at mature nodes of Ranvier in central and peripheral myelinated axons (Catterall et al., 2005; Meisler and Kearney, 2005). $Na_v1.6$ contributes to persistent current, resurgent current and repetitive firing in cerebellar Purkinje cells and DRG neurons (Raman et al., 1997; Cummins et al., 2005; Rush et al., 2005; Levin et al., 2006; Chen et al., 2008). Mutations of *Scn8a* in the mouse can result in tremor, ataxia, and other movement disorders (Meisler et al., 2004). Mice with null mutations in *Scn8a* exhibit paralysis and lethality by P21. A mutation of human *SCN8A* was identified in a family with ataxia and cognitive impairment (Trudeau et al., 2006).

The pore-forming α subunit of voltage-gated sodium channels is comprised of four homologous protein domains, each with six transmembrane segments, whose sequences are highly conserved in vertebrate and invertebrate channels. The 24 transmembrane segments contain residues affecting ion specificity, voltage dependence, and rates of activation and inactivation (Catterall et al., 2005). Most pathogenic missense mutations responsible for human sodium channelopathies are located in the transmembrane segments and adjacent cytoplasmic linkers (George, 2005; Kearney et al., 2006; Dib-Hajj et al., 2007). The ~130 residues of the sodium channel cytoplasmic N-terminal domain are also evolutionarily conserved, but few functions have been associated with this region of the protein. Five missense mutations in the N terminus of $Na_v1.1$, between residues 78 to 102, have been identified in patients with epilepsy (Fujiwara et al., 2003; Nabbout et al., 2003; Fukuma et al., 2004; Harkin et al., 2007). These patient mutations alter residues of the N terminus that are conserved in $Na_v1.6$, but the functional effects of the mutations have not been determined.

Screening of ENU-mutagenized mice for abnormal phenotypes and positional cloning of the mutated genes is an effective method for probing the *in vivo* functions of mammalian genes. We now report the positional cloning of an ENU-induced muta-

Received July 22, 2008; revised Dec. 18, 2008; accepted Jan. 15, 2009.

This work was supported by National Institutes of Health Grants R01 NS34509 (M.H.M.), U01 HD39372, and R01 CA115503 (M.J.J.), and a postdoctoral fellowship from the University of Michigan Center for Genetics in Health and Disease (L.M.S.). S.D.D.-H. and S.G.W. were supported by the Medical Research Service and Rehabilitation Research Service, Department of Veterans Affairs and by grants from the National Multiple Sclerosis Society. We thank Chris Dinh and Andrew Salinger for technical assistance with genetic mapping, and the Isom laboratory for advice regarding neuronal cell culture.

*S.D.D.-H. and M.H.M. contributed equally to this work.

Correspondence should be addressed to Miriam H. Meisler, 4909 Buhl Box 5618, University of Michigan, Ann Arbor, MI 48109-5618. E-mail: meislerm@umich.edu.

DOI:10.1523/JNEUROSCI.6026-08.2009

 0270-6474/09/292733-09$15.00/0

tion that causes juvenile lethality in the *ataxia3* mouse. Identification of a missense mutation in the cytoplasmic N terminus of $Na_v1.6$ provided an opportunity to investigate the cellular role of this domain of the sodium channel protein.

Materials and Methods

Animals. The ENU-induced neurological mutant *ataxia3* was generated in the Developmental Mutagenesis Program at the Baylor College of Medicine (Kile et al., 2003). The mutant is formally designated MGI: 2671787, nur^{m14Jus}. Mutagenesis was performed in strain C57BL/6J background, and the mutant stock is maintained by crossing heterozygotes to C57BL/6J mice to preserve the homogeneous genetic background.

Genetic mapping. Mapping was performed by crossing the mutant strain to the 129S6/SvEv inbred strain to the N2 generation. N2 siblings were intercrossed and DNA from 22 offspring were analyzed with microsatellite markers that map to all mouse autosomes and the X chromosome (Research Genetics). Significant linkage was detected to *D15Mit42*, and a total of 12 markers on Chromosome 15 were analyzed. Intercross statistics were evaluated using Map Manager QTL at $p = 0.01$ (Ken Manley, Roswell Park Cancer Institute, Buffalo, NY).

cDNA constructs. The plasmid pcDNA3-$Na_v1.6_R$ encodes the full-length mouse $Na_v1.6$ with the amino acid substitution Y371S that renders the channel resistant to micromolar concentrations of tetrodotoxin (TTX-R) (Herzog et al., 2003; Cummins et al., 2005). The S21P mutation (c.61T>C) was introduced into $Na_V1.6_R$ using the QuickChange XL II site-directed mutagenesis kit (Stratagene). The human $\beta1$ and $\beta2$ constructs (Lossin et al., 2002) were provided by Dr. A. L. George (Vanderbilt University, Nashville, TN).

Western blots. The membrane fraction was prepared from brain homogenates by centrifugation at 100,000 × *g* as previously described (West et al., 1992). Western blots loaded with 50 μg of membrane protein were stained with anti-$Na_v1.6$ antibody (1:200) from Sigma (S0438, lot 076K1101) as described (Levin and Meisler, 2004).

Northern blots. Northern blots contained 2 μg of polyA$^+$ RNA prepared from brain homogenates as previously described (Burgess et al., 1995). The probe was a ^{32}P-labeled RT-PCR product corresponding to exons 1–6 of mouse *Scn8a*.

Immunohistochemistry of sciatic nerve. Staining was performed as previously described (Kearney et al., 2002). Rabbit polyclonal anti-$Na_v1.6$ (Sigma, #S0438, antiserum lot 076K1101) was diluted 1:100. Anti-Caspr (University of California, Davis/ National Institute of Neurological Disorders and Stroke/National Institute of Mental Health NeuroMab Facility, clone K65/35) was diluted 1:1000. The secondary antibodies were biotinylated goat anti-rabbit IgG (1:250; Jackson Laboratories) and anti-mouse-Alexa-488 (1:500; Invitrogen). Polyclonal antibody labeling was visualized with strepavidin–Alexa-568 (1:400; Invitrogen). Images were captured with an Olympus FluoView 500 Laser Scanning Confocal Microscope in the University of Michigan Microscopy and Image Analysis Laboratory.

Cell transfections. The cell line ND7/23 was generated by fusion of DRG neurons with neuroblastoma cell line N18Tg2 (Wood et al., 1990). Wild type $Na_V1.6_R$ and $Na_V1.6_R$-S21P mutant constructs were transfected into ND7/23 cells using Lipofectamine 2000 (Invitrogen) as described previously (Wittmack et al., 2004). Briefly, ND7/23 cells were plated on 10 mm coverslips in 24-well plates, flooded with 0.5 ml of DMEM plus10% FBS and incubated at 37°C for 40 h. Cells were cotransfected with wild-type $Na_V1.6_R$ or S21P mutant constructs (0.8 μg/well) together with GFP (0.2 μg/well) (pEGFP, Clontech). Lipofectamine 2000 reagent (1.5 μl) and DNA (1 μg total) were each mixed with 50 μl of DMEM media (serum free, antibiotics free) and incubated at room temperature for 5 min. The two solutions were then combined and incubated at room temperature for 20 min. The mixture (100 μl per well) was added to the ND7/23 cell culture medium (0.5 ml of DMEM plus10% FBS per well) and incubated at 37°C for 3 h. After replacement with fresh DMEM supplemented by 10% FBS, the cells were incubated in 95% air-5% CO_2 for 18 h at 37°C or 30°C (low temperature) before electrophysiological measurements.

Electrophysiology. Whole-cell voltage-clamp recordings were performed at room temperature (20−22°C) using an Axopatch 200B amplifier (Axon Instruments). ND7/23 cells with robust green fluorescence signal were selected for patch-clamp. Fire-polished electrodes (0.6–1.3 MΩ) were fabricated from 1.6 mm outer diameter borosilicate glass micropipettes (World Precision Instruments). The pipette potential was adjusted to zero before seal formation, and liquid junction potential was not corrected. Capacity transients were canceled and voltage errors were minimized with 80% series resistance compensation. Currents were acquired with Clampex 9.2 at 6 min after establishing whole-cell configuration, sampled at a rate of 50 or 100 kHz, and filtered at 5 kHz.

For current-voltage relationships, cells were held at −120 mV and stepped to a range of potentials (−65 to + 60 mV in 5 mV increments) for 100 ms each. Peak inward currents (I) were plotted as a function of depolarizing potential to generate *I–V* curves. Activation curves were obtained by converting current (I) to conductance (G) at each voltage (V) using the equation $G = I/(V - V_{rev})$, where V_{rev} is the reversal potential which was determined for each cell individually. Activation curves were then fit with Boltzmann function in the form of $G = G_{max}/(1 + \exp[(V_{1/2,act} - V)/k])$, where G_{max} is the maximal sodium conductance, $V_{1/2,act}$ is the potential at which activation is half-maximal, V is the test potential, and k is the slope factor.

Steady-state fast inactivation was achieved with a series of 500 ms prepulses (−140 to −10 mV in 10 mV increments), and the remaining available channels were activated by a 20 ms test pulse to −10 mV. Peak inward currents obtained from steady-state fast-inactivation protocols were normalized to the maximal peak current (I_{max}) and fit with Boltzmann functions: $I/I_{max} = 1/(1 + \exp[(V - V_{1/2,inact})/k])$, where V represents the inactivating prepulse potential, $V_{1/2,inact}$ represents the midpoint of inactivation curve.

The pipette solution contained (in mM): 140 CsF, 10 NaCl, 1 EGTA, 10 dextrose, and 10 HEPES, pH 7.35 (adjusted with CsOH), and the osmolarity was adjusted to 315 mOsmol/L with sucrose. The extracellular bath solution contained (in mM): 140 NaCl, 3 KCl, 1 $MgCl_2$, 1 $CaCl_2$, 20 TEACl, 5 CsCl, 0.1 $CdCl_2$, 10 HEPES, pH 7.35 (adjusted with NaOH), and the osmolarity was 328 mOsmol/L. Tetrodotoxin (TTX; 300 nM) was added to the bath solution to block endogenous voltage-gated sodium currents in ND7/23 cells (Zhou et al., 2003; John et al., 2004; Wittmack et al., 2004; Rush et al., 2005; Wittmack et al., 2005), permitting currents from wild type $Na_v1.6$ or S21P mutant channels to be recorded in isolation.

Data analysis. Data were analyzed using Clampfit 9.2 (Molecular Devices) and Origin 7.5 (Microcal Software), and presented as means ± SE. The Kruskal–Wallis nonparametric test was used to analyze current density data. One way ANOVA was used to assess the statistical significance of changes in characteristics of channel activation and inactivation.

Gradient isolation and culture of cerebellar granule cells. Cerebellar granule cells were prepared and cultured from 14- to 18-d-old mice (P14–18) by modification of previously described methods (Brewer, 1997). Each brain was removed and placed in 2 ml of ice-cold Hibernate A (BrainBits) supplemented with B27 (Invitrogen) and 0.5 mM L-glutamine. The cerebellum was dissected and diced into smaller pieces. The tissue was incubated in a warm trypsin/Hibernate solution for 30–40 min with agitation every 5–10 min, and then transferred to 2 ml of fresh HibernateA/B27/L-glutamine and triturated 10 times with a P1000 pipette tip. After addition of 2 ml of HibernateA/B27/L-glutamine, the tissue was allowed to settle. Aliquots (2 ml) of supernatant were removed to a 15 ml conical tube. Trituration was repeated 3 times. 8 ml of the triturated cell suspension was placed on a 4 ml step gradient prepared from 1 ml aliquots of 35%, 25%, 20% and 15% (v/v) Optiprep (Sigma): HepesNaCl, 1:1, in HibernateA/B27/L-glutamine. The cell suspension was centrifuged at 800 × g for 15 min. Cell debris floating above the 4 ml gradient was discarded. The bottom two 2 ml, excluding the pellet, were resuspended in 12 ml of NeurobasalA Full media (Neurobasal A/0.5 mM L-glutamine). To 50 ml of suspension was added 1 ml of B27 supplement, 10 μl 50 mg/ml gentamicin and 2.5 μl of b-FGF (Invitrogen) prepared by resuspending 10 μg of b-FGF in 100 μl 10 mM Tris pH 1.7 containing 0.1% BSA. The suspension was centrifuged at 1500 × g and the cell pellet was resuspended in 4 ml of Neurobasal A Full media. The cells were

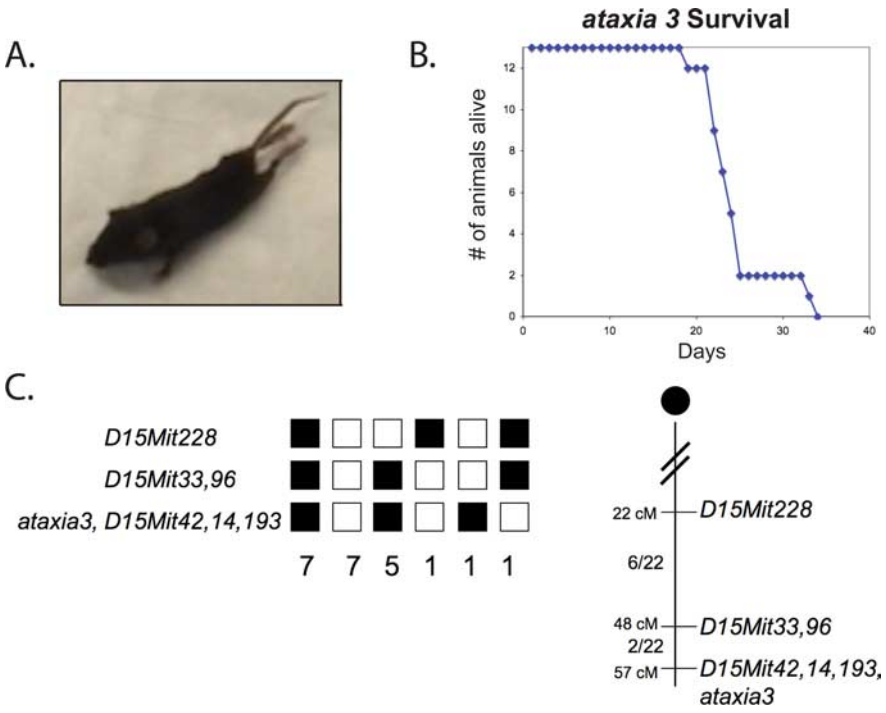

Figure 1. Phenotype and mapping of the *ataxia3* mutant. ***A***, Impaired hindlimb function in *ataxia3* homozygote. ***B***, Juvenile lethality of the *ataxia3* homozygote. ***C***, the *ataxia3* mutation maps to the distal region of mouse chromosome 15. The haplotypes for 22 chromosomes from 11 F2 mice are indicated. Solid symbols, B6 alleles; open symbols, 129 alleles. The *ataxia3* mutation did not recombine with the markers *D15Mit193, D15Mit42* and *D15Mit14*.

plated on glass coverslips coated with poly-L-lysine (Sigma) and laminin (Sigma) and incubated at 37°C, 5% CO_2. Seventy-five percent of the medium was changed 24 h after isolation and this was repeated every 3–4 d.

Immunohistochemistry of cerebellar granule cells. Neurons were fixed in 4% PFA in PBS for 15 min with rocking at room temperature, washed, and permeabilized in 0.1% Triton, 6% BSA for 30 min at room temperature. The cells were blocked in 10% normal goat serum in PBS for 30 min at room temperature. All antibodies were diluted in Wash Buffer (1% BSA, 0.1% Triton X-100 in PBS). Primary antibodies were incubated overnight with rocking at 4°C. Secondary antibodies were incubated at room temperature for 1 h. Although the rabbit polyclonal anti-Na_v1.6 (Sigma #SO438) generates specific staining of nodes of Ranvier (see above and Kearney et al., 2002), this antibody produced high background staining of null cerebellar granule cells that lack Na_v1.6 (supplemental Fig. 1, available at www.jneurosci.org as supplemental material). Therefore, mouse Na_v1.6 in cultured cells was detected with anti-Na_v1.6 Na^+ channel, clone K87A/10 mouse monoclonal IgG (Neuromab Facility, lot number: 440-8HK-09) used at 1:100 dilution. The secondary antibody was anti-mouse-Alexa-488 (1:500; Invitrogen). The ER marker, protein disulfide isomerase (PDI), was detected with rabbit PDI Polyclonal Antibody (Assay Designs) used at 1:500 dilution. The secondary antibody was goat-anti-rabbit Alexa 594 (1:800, Invitrogen). The *cis*-Golgi marker, GM130, was detected with mouse monoclonal anti-GM130 used at 1:20 dilution (BD Transduction Laboratories). The secondary antibody was goat-anti-mouse Alexa 594 (1:800, Invitrogen). For double-labeling with monoclonal anti-Na_v1.6 and monoclonal GM130, the anti-Na_v1.6/Alexa 488 staining was completed first and followed by anti-GM130/Alexa 594 staining. Neurofilament-200 was detected with polyclonal anti-Neurofilament-200 (Sigma, product no. N 4142) used at 1:80 dilution. The secondary antibody was goat-anti-rabbit Alexa 594 (1:800, Invitrogen). Cell nuclei were stained with 1 μg/ml DAPI (Invitrogen) in PBS for 15 min. Coverslips were mounted on microscope slides with Prolong Gold (Invitrogen) and dried overnight. Images were captured with an Olympus FluoView 500 Laser Scanning Confocal Microscope in the University of Michigan Microscopy and Image Analysis Laboratory.

Results

Phenotype of the *ataxia3* mutant

The *ataxia3* mutant was identified in a large-scale mutagenesis program after administration of the mutagen ENU to mice of strain C57BL/6J. A G3 breeding scheme was used to detect recessive mutations with visible phenotypes (Kile et al., 2003). The *ataxia3* mutant was recognized by its locomotor abnormalities that include pronounced tremor, ataxic gait, and partial loss of hindlimb function. Affected animals have impaired use of their hindlimbs by 2 weeks of age (Fig. 1*A*), and do not survive beyond 1 month (Fig. 1*B*). In the initial crosses between heterozygous carriers, we observed 27 affected animals among a total of 106 offspring, consistent with autosomal recessive inheritance and complete penetrance of the phenotype ($p = 0.99$).

Genetic mapping of *ataxia3* to mouse chromosome 15

To map the mutation, C57BL/6J.*ataxia3*/+ heterozygotes were crossed to strain 129S6/SvEvTac for two generations. Heterozygous mice from the N2 generation were intercrossed. Twenty-two offspring from the intercross were genotyped with microsatellite markers. The *ataxia3* locus was nonrecombinant with three markers on distal chromosome 15: *D15Mit193*, *D15Mit42* and *D15Mit14* (Fig. 1*C*). The observed gene order and recombination distances (cM ± SE) were as follows: *D15Mit228* - 14 ± 5 - *D15Mit33,D15Mit96* - 4.6 ± 3 - *ataxia3,D15Mit42,D15Mit14,D15Mit193*.

Identification of a mutation in *Scn8a* encoding sodium channel Na_v1.6

The nonrecombinant markers for the *ataxia3* locus are located between 55 and 58 cM on mouse chromosome 15, while the *Scn8a* gene encoding Na_v1.6 is located at 60 cM. The tremor, ataxia, and hindlimb impairment in *ataxia3* mice strongly resemble the phenotypes of known mutants of *Scn8a* (Meisler et al., 2004). We therefore evaluated *Scn8a* as a positional candidate gene for *ataxia3*. The Na_v1.6 cDNA was amplified by RT-PCR as previously described (Buchner et al., 2004) and the products were gel-purified and sequenced. The nucleotide substitution c.61T>C (GenBank NM_001077499) was identified in the *ataxia3* cDNA (Fig. 2*A*). The destruction of a *Hinf*1 site by the T>C mutation can be used for genotyping the mutant mice (Fig. 2*C*). The resulting substitution of serine residue 21 by proline (p.S21P) is located close to the N terminus of the channel (Fig. 2*B*). Serine residue 21 is evolutionarily conserved in vertebrate sodium channels including the muscle channel Na_v1.4 and the cardiac channel Na_v1.5, and also in invertebrate sodium channels, suggesting a conserved function common to these channels (Fig. 2*D*). The retention of some hindlimb function in the *ataxia3* mice (see above) indicates that Na_v1.6-S21P is not a null allele, since the null mice develop complete paralysis of the hindlimbs (Meisler et al., 2004).

Noncomplementation of *ataxia3* and a null allele of *Scn8a*

To demonstrate that the Na$_v$1.6-S21P mutation is responsible for the mutant phenotype of the mice, we tested the ability of the mutant allele to complement the recessive lethality of the null allele *Scn8a*^{tg1} (Burgess et al., 1995). Heterozygous *ataxia3*/+ mice were crossed with null heterozygotes. The *Scn8a*$^{S21P/tg1}$ compound heterozygotes were born in the predicted Mendelian ratio of 24% (5/22) but none of the compound heterozygotes survived beyond weaning. All of the compound heterozygotes exhibited the tremor and ataxia that are characteristic of each homozygous mutant. The failure of the *ataxia3* mutant to rescue the motor abnormalities and lethality of a null allele of *Scn8a*, together with the phenotypic similarity of *ataxia3* to *Scn8a* mutants and the genetic mapping of *ataxia3* near *Scn8a*, strongly support the identification of Na$_v$1.6-S21P as the causal mutation in *ataxia3* mice.

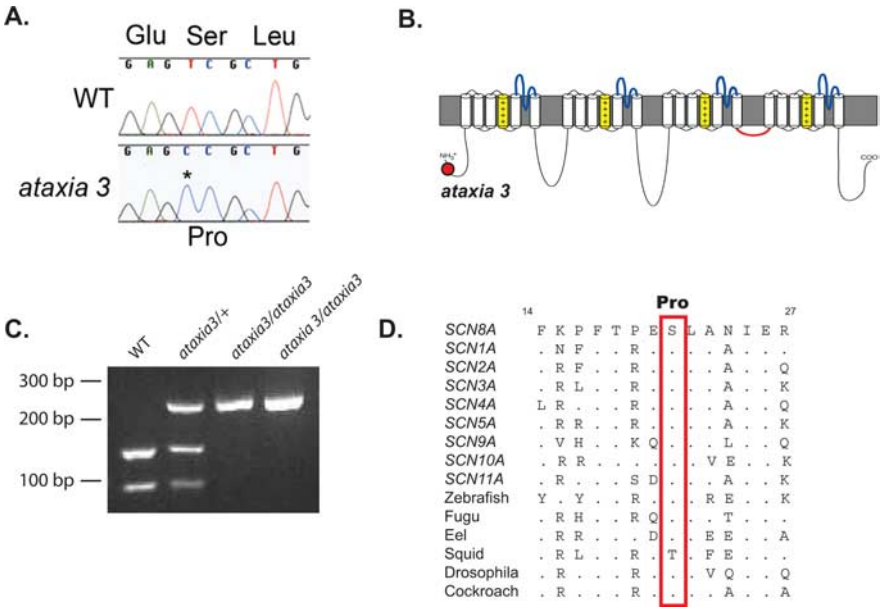

Figure 2. The *ataxia3* mutation causes a Ser−>Pro substitution at a conserved residue of Na$_v$1.6. ***A***, Sequence chromatogram demonstrating the T−> C mutation in *ataxia3*. ***B***, Location of S21P in the cytoplasmic N-terminal domain of Na$_v$1.6. ***C***, Genotyping assay based on loss of a *Hinf*1 restriction site due to the T>C mutation in *ataxia3*. ***D***, Evolutionary conservation of serine 21 in the human sodium channel gene family (*SCN1A-SCN11A*) and invertebrate sodium channels.

Abundance and localization of Na$_v$1.6-S21P in mutant mice

To determine whether the c.61T>C mutation destabilizes the *Scn8a* transcript, we prepared a Northern blot with polyA$^+$ RNA from brain and hybridized it with a Na$_v$1.6 cDNA probe. The size and abundance of the 10 kb mRNA were comparable in the wild-type and homozygous *ataxia3* RNA (Fig. 3*A*). Both samples also contain the minor *Scn8a* transcript of 12 kb that terminates at an alternative polyadenylation site (Drews et al., 2005)

To examine the abundance of the Na$_v$1.6 channel protein, membrane protein was purified from *ataxia3* and wild-type mouse brain. Western blotting with anti-Na$_v$1.6 antibody detected a low level of full-length Na$_v$1.6 protein in homozygous *ataxia3* brain (Fig. 3*B*). The protein is not detected in the null control (Fig. 3*B*). The abundance of Na$_v$1.6 protein in the homozygous *ataxia3* mutant is greatly reduced in comparison with heterozygote and wild-type brain (Fig. 3*B*).

To determine whether Na$_v$1.6-S21P is present at the nodes of Ranvier, where the normal channel is highly concentrated, sciatic nerves were dissected, teased onto poly-L-lysine coated coverslips and immunostained for Na$_v$1.6 and the paranodal marker Caspr as previously described (Kearney et al., 2002). Nodal Na$_v$1.6 was readily detected in nerves from *ataxia3*/+ heterozygotes that produce 50% of the normal level of wild-type channel (Fig. 3*C*). In contrast, Na$_v$1.6 protein could not be detected at any nodes in sciatic nerve from *ataxia3* mice (Fig. 3*C*). As a control, we were able to detect Na$_v$1.6 in nodes from sciatic nerve of *Scn8a*$^{medJ/medJ}$ mice which produce 10% of the wild-type level of channel protein (Fig. 3*C*) (Kearney et al., 2002). The absence of Na$_v$1.6 at the nodes of Ranvier in *ataxia3* mice is consistent with a defect in trafficking of the S21P protein.

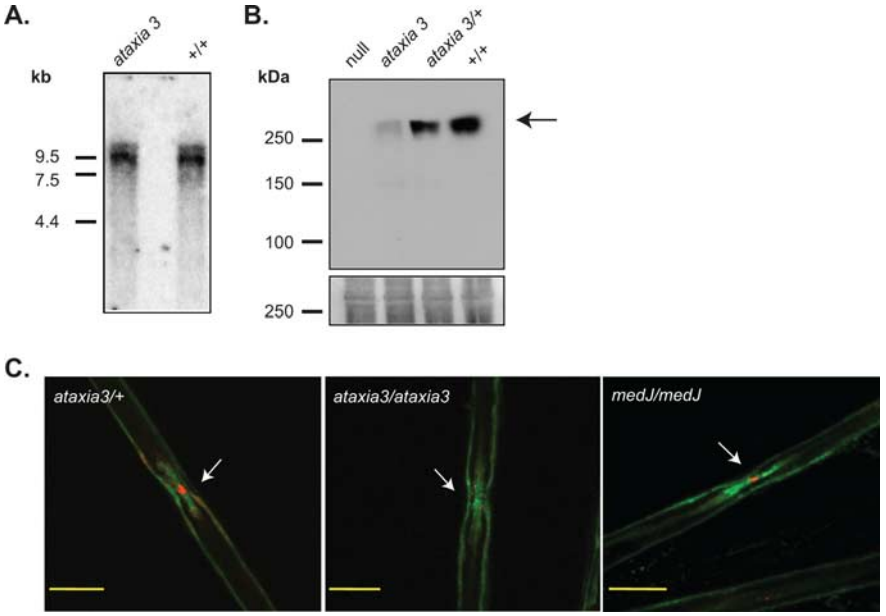

Figure 3. Na$_v$1.6 transcript and protein in *ataxia3* mice. ***A***, A Northern blot containing 3 μg of polyA$^+$ RNA from wild-type and homozygous *ataxia3* brain was hybridized with a radiolabeled 1 kb cDNA fragment from Na$_v$1.6. ***B***, Western blot containing 50 μg of membrane protein from wild-type and homozygous *ataxia3* brain homogenates was stained with polyclonal anti-Na$_v$1.6 antiserum as described (Levin and Meisler, 2004). The blot was stained with Ponceau S to visualize total protein (bottom). ***C***, Na$_v$1.6 at nodes of Ranvier. Teased sciatic nerve was stained with polyclonal anti-Na$_v$1.6 antiserum as described (Kearney et al., 2002). Red, anti-Nav1.6; green, anti-Caspr. Images were captured with an Olympus FluoView 500 Laser Scanning Confocal Microscope. As a quantitative positive control, nodal Na$_v$1.6 is visible in the homozygous *medJ* mutant in which channel protein is reduced to 10% of wild-type levels (Kearney et al., 2002; Buchner et al., 2003).

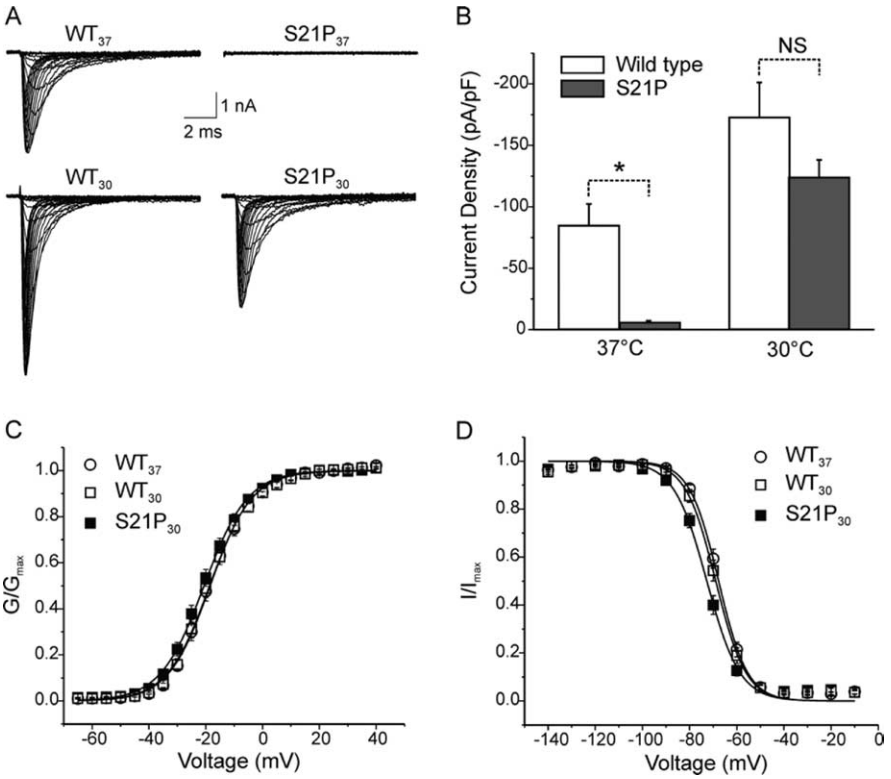

Figure 4. Electrophysiological characterization of $Na_V1.6$ in ND7/23 cells. ***A***, Representative family traces of Na^+ currents from ND7/23 cells transfected with either wild-type $Na_V1.6_R$ or $Na_V1.6_R$-S21P mutant channels. WT_{37}, wild-type channel and incubation at 37°C; $S21P_{37}$, mutant channel and incubation at 37°C; WT_{30}, wild-type channel and cells incubated at 30°C; $S21P_{30}$, mutant channel and cells incubated at 30°C. Cells were held at −120 mV and Na^+ currents were elicited by step depolarizations from −65 to + 60 mV in 5 mV increments every 5 s. ***B***, Peak current densities of wild-type $Na_V1.6_R$ and S21P channels in cells that were incubated at 37°C or 30°C. WT_{37}, $n = 30$; $S21P_{37}$, $n = 18$; WT_{30}, $n = 21$; $S21P_{30}$, $n = 28$). ***C***, Boltzmann's fit for voltage-dependent activation of Na^+ currents from ND7/23 cells transfected with wild-type $Na_V1.6_R$ channels at 37°C ($n = 12$) and 30°C ($n = 13$); and S21P mutant channels at 30°C ($n = 17$). ***D***, Boltzmann's fit for voltage-dependent steady-state fast inactivation of Na^+ currents from ND7/23 cells transfected with wild-type $Na_V1.6_R$ channels and incubated at 37°C ($n = 12$) or 30°C ($n = 13$), and S21P mutant channels from cells incubated at 30°C ($n = 17$). Cells were held at −120 mV and a series of 500 ms prepulses from −140 mV to −10 mV were evoked followed by 40 ms test pulses to −10 mV.

Channel activity in transfected ND7/23 cells

Electrophysiological measurement of channel activity is a sensitive method for detection of functional sodium channels at the cell surface. To determine whether functional $Na_v1.6$-S21P channels are present at the cell membrane, we used an assay in which ND7/23 cells, a DRG-derived cell line, are transfected with a TTX-resistant version of wild-type $Na_v1.6$ cDNA ($Na_V1.6_R$) with the amino acid substitution Y371S (Herzog et al., 2003). In the presence of 300 nM TTX, endogenous sodium currents in ND7/23 cells are blocked and currents derived from the transfected wild-type $Na_V1.6_R$ and its derivatives can be studied in isolation (see Materials and Methods).

ND7/23 cells were cotransfected with EGFP and $Na_V1.6_R$ or the derivative $Na_V1.6_R$-S21P and analyzed by whole-cell voltage clamp electrophysiology. Transfected cells with robust green fluorescence were recorded. All cells that formed whole-cell configuration were included in the calculation of current density, with peak current measured at −5 mV. Activation and inactivation properties were analyzed for the subset of cells with large currents ($I_{Na} > 1$ nA).

Most (26/30) cells transiently transfected with wild type $Na_v1.6_R$ and incubated at 37°C produced a TTX-R current >200 pA, the smallest Na current that could be unequivocally attributed to the recombinant sodium channels. The $Na_v1.6_R$ channels exhibited the expected current-voltage relationship (Fig. 4*A*). The average peak current density of wild-type $Na_V1.6_R$ channels at −5 mV was 84.9 ± 17.5 pA/pF ($n = 30$) (Fig. 4*B*), with $V_{1/2}$ of activation −18.3 ± 1.2 mV and $V_{1/2}$ of steady-state fast inactivation of −67.7 ± 1.0 mV ($n = 12$) (Fig. 4*C*), in agreement with our previous reports (Wittmack et al., 2004, 2005; Rush et al., 2005).

In contrast to the observations with the wild-type construct, 17 of 18 cells transfected with S21P mutant channels failed to produce currents >200 pA (Fig. 4*A*,*B*). One cell produced a 550 pA peak current, resulting in an average peak current density for S21P mutant channels of 5.8 ± 1.5 pA/pF (mean ± SE) ($n = 18$).

We tested the ability of cotransfected β1 and β2 subunits to rescue the channel activity of the S21P construct. The majority of ND7/23 cells transfected with wild-type $Na_v1.6$, β1 and β2 subunits (7 of 8) produced sodium currents with average current density = 86.7 ± 21.8 pA/pF ($n = 8$). In contrast, only 2 of 14 cells expressing $Na_V1.6_R$-S21P produced sodium currents, and the average current density was only 6.9 ± 0.8 pA/pF ($n = 14$). Thus overexpression of β1 and β2 subunits did not rescue the activity of $Na_V1.6$-S21P mutant channels. These experiments indicate that under physiological conditions, $Na_v1.6$-S21P does not exhibit channel activity, possibly due to failure to reach the cell surface.

Rescue of $Na_V1.6$-S21P channel activity at low temperature (30°C)

Incubation of cells at lower temperature can permit the production of functional protein from mutants that are defective in protein folding or transport (Ulloa-Aguirre et al., 2004; Rusconi et al., 2007). To test the hypothesis that impaired trafficking is responsible for the lack of functional $Na_v1.6$-S21P channels at the cell surface at 37°C, we incubated ND7/23 cells at 30°C for 18 h after transfection with the mutant cDNA. The reduction in incubation temperature did not alter the level of functional wild-type $Na_V1.6_R$, and 19/21 transfected cells produced voltage-dependent inward currents with an average peak current density of 173.1 ± 28 pA/pF ($n = 21$) (Fig. 4*A*,*B*). Under these culture conditions, the S21P mutant channel also exhibited robust activity: 26 of 28 transfected cells generated voltage-dependent inward currents with an average peak current density of 123.8 ± 14.3 pA/pF ($n = 28$) (Fig. 4; Table 1). The restoration of channel activity at 30°C is consistent with the model that $Na_v1.6$-S21P retains normal biophysical properties, but the channel is not transported to the cell surface at 37°C.

Analysis of Boltzmann fits for channel activation and steady-state fast inactivation of WT channels did not show a temperature-dependent effect on these properties. No significant difference was observed on the voltage dependence of activation and steady-state fast inactivation of WT channels at 30°C ($V_{1/2,activation} = -18.6 \pm 1.2$ mV, $V_{1/2,inactivation} = -69.0 \pm 1.1$

mV, $n = 13$) (Fig. 4*C*,*D*), compared with the values at 37°C (Table 1). The S21P mutation did not change the voltage dependence of channel activation ($V_{1/2,activation} = -20.5 \pm 1.1$ mV, $n = 17$) (Fig. 4*C*) compared with WT channels. However the S21P mutation caused a small but statistically significant −3.7 mV hyperpolarizing shift in steady-state fast inactivation (Fig. 4*D*) ($V_{1/2,inactivation} = -72.7 \pm 1.1$ mV, $n = 17$, $p < 0.05$ vs wild-type $Na_V1.6_R$ at 30°C).

Table 1. Summary of electrophysiological characterization of wild-type $Na_v1.6$ and S21P mutant channels

	pA/pF	$V_{1/2,activation}$ (mV)	$V_{1/2,fast\ inact}$ (mV)
Wild type at 37°C	−84.9 ± 17.5(n= 30)	−18.3 ± 1.2 (n = 12)	−67.7 ± 1.0 (n = 12)
S21P at 37°C	−5.8 ± 1.5 (n=18)*	Not applicable	Not applicable
Wild type at 30°C	−173 ± 28 (n= 21)	−18.6 ± 1.2 (n = 13)	−69.0 ± 1.1 (n = 13)
S21P at 30°C	−124 ± 14 (n= 28)	−20.5 ± 1.1 (n = 17)	−72.7 ± 1.1 (n = 17)*

ND7/23 cells were transfected with $Na_v1.6_R$ wild-type or S21P mutant constructs and incubated at 37°C or 30°C for 18 h before recording TTX-R sodium currents. Values represent mean ± SEM for the indicated number of recorded cells. *Significant difference ($p < 0.05$) between mutant and wild-type channels.

Subcellular localization of mutant $Na_v1.6$-S21P protein

To determine the intracellular location of $Na_v1.6$-S21P protein that fails to reach the cell surface we isolated cerebellar granule cells from *ataxia3* and wild-type mice at P14–18 and maintained them in culture at 37°C for 16 d. During this period, isolated neurons redifferentiate and regenerate neuronal processes and their components (Osorio et al., 2005; Van Wart and Matthews, 2006).

After 1 week in culture, both wild-type and mutant $Na_v1.6$ protein colocalized with the *cis*-Golgi marker GM130 (Fig. 5*A*). This localization is consistent with the high carbohydrate content of voltage-gated sodium channels (Waechter et al., 1983; Schmidt and Catterall, 1987). Neither wild-type nor mutant $Na_v1.6$ was colocalized with the endoplasmic reticulum marker α-protein disulfide isomerase (PDI) (Fig. 5*B*). These data indicate that $Na_v1.6$-S21P escapes the ER quality control system and is transported to the Golgi apparatus during biosynthesis.

After 16 d in culture, abundant neuronal processes were detected in both wild-type and mutant cultures by staining for neurofilament-200 (Fig. 6*A*, left panel). In the wild-type neurons (401 of 717), most of the $Na_v1.6$ protein was located in the cell soma and processes, while in the *ataxia3* neurons (263 of 279), the $Na_v1.6$-S21P retained a perinuclear localization (Fig. 6*A*, middle and right panels). Costaining with the *cis*-Golgi marker GM130 confirmed the complete retention of $Na_v1.6$-S21P in the Golgi apparatus (Fig. 6*B*). The data demonstrate failure of anterograde transport of $Na_v1.6$-S21P out of the Golgi complex. This biosynthetic defect can account for the failure $Na_v1.6$-S21P to reach the cell surface in transfected cells and its absence from nodes of Ranvier *in vivo*.

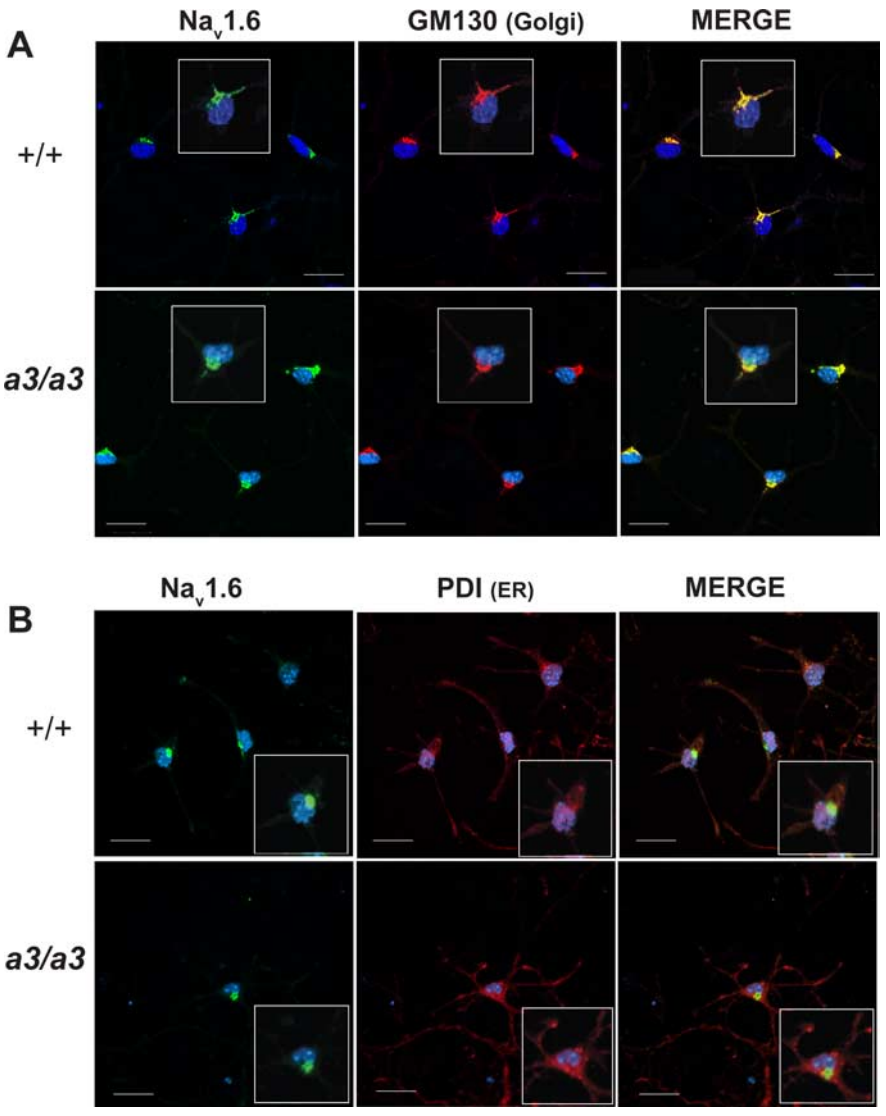

Figure 5. Subcellular localization of $Na_v1.6$ in cerebellar granule cells after 1 week of culture. ***A***, Costaining of $Na_v1.6$ (green) and GM130, a marker for the *cis*-Golgi (red). ***B***, Costaining of $Na_v1.6$ (green) and α-protein disulfide isomerase (PDI), a marker of the endoplasmic reticulum (ER) (red). Cell nuclei are stained with DAPI (blue). Images were captured with an Olympus FluoView 500 Laser Scanning Confocal Microscope. Scale bars, 20 μm. a3, *ataxia3*.

Discussion

We have identified and characterized a novel missense mutation of mouse *Scn8a*, p.Ser21Pro, that results in juvenile lethality *in vivo*. S21P is located in an evolutionarily conserved portion of the cytoplasmic N-terminal domain that is present in neuronal, cardiac and muscle channels and in invertebrate sodium channels, suggesting that this domain participates in a cellular function that is common to all of these sodium channels. Our evidence for a role in intracellular trafficking is consistent with this expectation. The mutated serine residue 21 is located at one end of a predicted α helix (www.predictprotein.org), and substitution of proline for serine at this position could destabilize the helix. Alternatively this mutation may eliminate a site of protein phosphorylation, although the surrounding sequence is not a good match for any

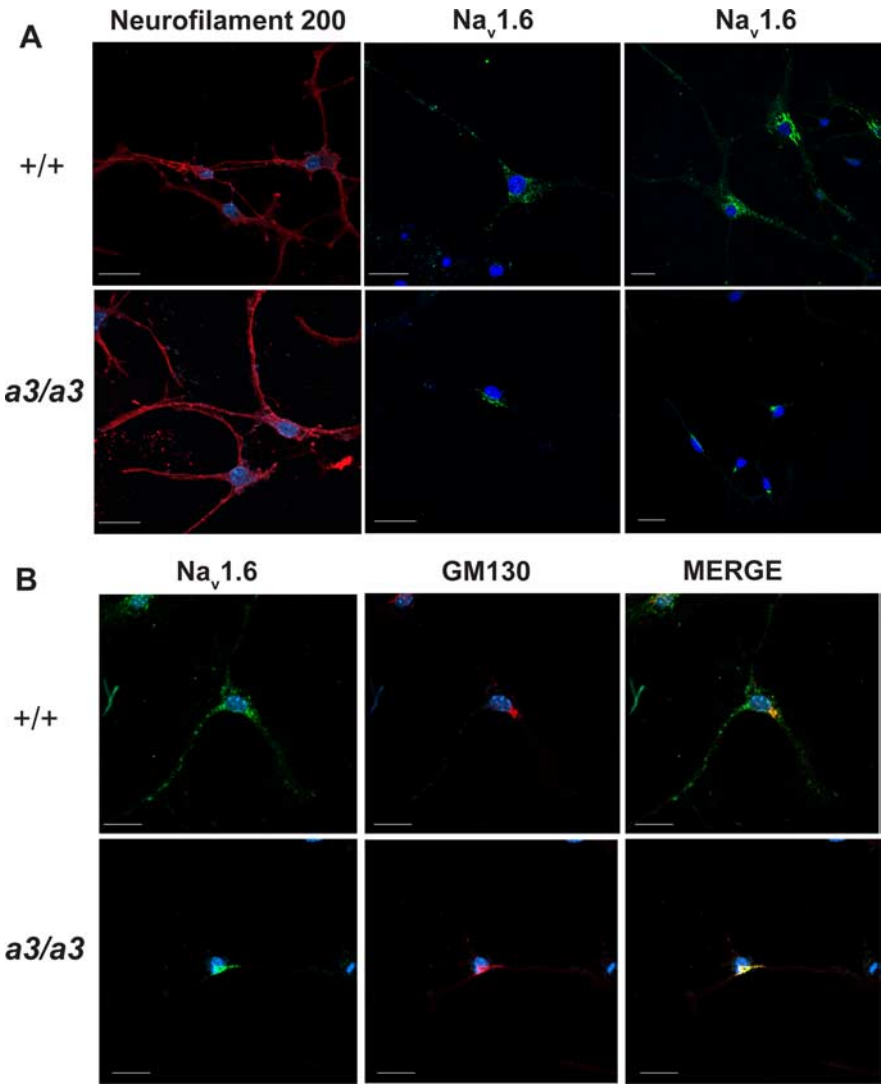

Figure 6. Subcellular localization of Na_v1.6 in cerebellar granule cells after 16 d of culture. ***A***, left panel, abundant neuronal processes in wild-type and *ataxia3* mutant cells visualized by staining for neurofilament. middle and right, representative images of wild-type and mutant cells. ***B***, Costaining of Na_v1.6 (green) and the *cis*-Golgi marker (red). In the mutant *ataxia3* cells, Na_v1.6 remains localized in the Golgi. Cell nuclei are stained with DAPI (blue). Images were captured with an Olympus FluoView 500 Laser Scanning Confocal Microscope. Scale bars, 20 μm. a3, *ataxia3*.

consensus motif for protein phosphorylation, with a predicted phosphorylation potential of only 0.14 (http://ca.expasy.org). Full-length Na_v1.6-S21P protein was detected at reduced abundance on Western blots, but it could not be detected at nodes of Ranvier by immunostaining. In transfected cells, Na_v1.6-S21P did not exhibit channel activity at 37°C, but activity was rescued when transfected cells were maintained at 30°C. The data are consistent with the view that the mutant protein is trapped within an intracellular compartment at 37°C and does not reach the cell membrane.

Pathogenic mutations that impair intracellular trafficking have been identified of the cardiac channel *SCN5A* (Na_v1.5) in patients with Brugada syndrome (Valdivia et al., 2004; Poelzing et al., 2006; Tan et al., 2006) and the neuronal channel *SCN1A* (Na_v1.1) in a patient with Severe Myoclonic Epilepsy of Infancy (Rusconi et al., 2007). These mutations were not located in the N-terminal domain, and were shown to result in reduced or absent inward sodium currents in heterologous expression systems such as HEK 293 cells. The channel activity of these mutants has been rescued by incubation of transfected cells at reduced temperatures, treatment with channel blockers, or over-expression of β-subunits (Valdivia et al., 2004; Poelzing et al., 2006; Tan et al., 2006; Pfahnl et al., 2007; Rusconi et al., 2007). Lowering the incubation temperature is thought to slow the kinetics of protein folding, allowing more time for the mutant proteins to acquire a functional conformation before sorting to the cell membrane (Ulloa-Aguirre et al., 2004). In the case of the Na_v1.6-S21P mutation, lower temperature appeared to rescued protein trafficking while overexpression of β-subunits did not.

To determine the fate of the mutant Na_v1.6-S21P protein, we examined primary cultures of cerebellar granule cells from *ataxia3* and wild-type mice. In wild-type neurons after 1 week in culture, most of the Na_v1.6 protein was located in the Golgi complex. This is the first demonstration that Na_v1.6, which is thought to be a glycoprotein, accumulates in the Golgi during redifferentiation of immature neurons in culture. After an additional 9 d in culture, wild-type Na_v1.6 was distributed throughout the soma and neuronal processes, while Na_v1.6-S21P was completely retained in the Golgi apparatus. These observations lead to the specific hypothesis that mutation of the cytoplasmic N-terminal domain prevents anterograde trafficking of channel protein out of the *cis*-Golgi, perhaps by preventing association with protein chaperones. Chaperones involved in the processing of sodium channels in the Golgi have not been identified, and the Na_v1.6-S21P mutant will be a useful reagent for identifying the interacting protein(s) required for anterograde transport of Na_v1.6 from the Golgi complex to the cell membrane.

Mutations in the N terminus of two other ion channels have been associated with retention in the Golgi. Deletion of residues 1–76 from the N terminus of Kir2.1 results in Golgi accumulation (Stockklausner and Klocker, 2003). Amino acid substitutions at residues 12 and 13 of the α-adrenergic receptor protein also prevented delivery to the cell surface and resulted in accumulation in the Golgi (Dong and Wu, 2006). Comparison of the primary sequences of these three channels did not identify a shared N-terminal sequence.

Accessory proteins that bind to the cytoplasmic domains of sodium channels can influence channel density at the cell surface (Cusdin et al., 2008). Binding of annexin II light chain (p11) between residues 74 and 103 of the N terminus of Na_v1.8 (Poon et al., 2004) increases the channel density at the surface of DRG neurons (Okuse et al., 2002). Binding of FGF13, a member of the fibroblast growth factor family, to the C terminus of Na_v1.6 also results in increased current density (Wittmack et al., 2004). β subunit binding sites are present in the extracellular portion of domain 4 (Catterall et al., 2005) as well as the cytoplasmic C

terminus (Spampanato et al., 2004), and interaction with β subunits can enhance targeting and trafficking of sodium channel α subunits to the cell surface (Chen et al., 2002, 2004; Lopez-Santiago et al., 2006). A trafficking-defective mutation in the C terminus of $Na_v1.1$ was rescued by overexpression of β subunits (Rusconi et al., 2007). The lack of rescue of $Na_v1.6$-S21P by β subunits indicates that the N terminus interacts with a different class of proteins.

This work has demonstrated that the neuromuscular disorder in *ataxia3* mice is a consequence of deficiency of $Na_v1.6$ at the cell membrane, resulting from retention in the Golgi complex. In contrast to $Na_v1.6$ null mice, which exhibit complete hindlimb paralysis, the *ataxia3* mutants retain a small amount of hindlimb function, suggesting that there is a low level of functional $Na_v1.6$-S21P *in vivo*. This is consistent with the observation of channel activity in a small proportion of cells transfected with the mutant channel at 37°C, and the detection of a small amount of channel protein on Western blots of membrane protein from mutant brain. The amount of functional protein *in vivo* can be estimated by comparison with other *Scn8a* mutants. Mice with the genotype *Scn8a*$^{medJ/medJ}$ produce 10% of normal $Na_v1.6$ and survive to adulthood (Kearney et al., 2002; Meisler et al., 2004). Mice with the genotype *Scn8a* $^{medJ/medJ}$, *Scnm1*$^{R187X/R187X}$ produce 5% of normal channel protein and do not survive beyond 3 weeks, but they do retain partial hindlimb function like the *ataxia3* mice (Kearney et al., 2002). Mice with 1.5% of normal levels of $Na_v1.6$ exhibit complete hindlimb paralysis and lethality at 3 weeks (Howell et al., 2008) (Howell et al., 2008). The phenotype of the *ataxia3* mice suggests that ~5% of $Na_v1.6$-S21P reaches the cell surface *in vivo*.

The identification of a mutation that impairs transport of $Na_v1.6$ out of the Golgi complex opens several new avenues of investigation. It will be feasible to screen for proteins whose interaction with the N terminus is prevented by the S21P mutation, and to determine whether trafficking of the mutant channel from the Golgi is rescued by sodium channel blockers such as phenytoin, lidocaine or mexiletine that can function as pharmacological chaperones in cultured cells (Valdivia et al., 2004; Rusconi et al., 2007; Zhao et al., 2007). The *ataxia3* mutation defines a new function of the cytoplasmic N terminus of $Na_v1.6$ and provides an *in vivo* model for testing pharmacological rescue of ion channelopathies caused by trafficking defects.

References

Brewer GJ (1997) Isolation and culture of adult rat hippocampal neurons. J Neurosci Methods 71:143–155.

Buchner DA, Trudeau M, Meisler MH (2003) SCNM1, a putative RNA splicing factor that modifies disease severity in mice [see comment]. Science 301:967–969.

Buchner DA, Seburn KL, Frankel WN, Meisler MH (2004) Three ENU-induced neurological mutations in the pore loop of sodium channel Scn8a (Na (v) 1.6) and a genetically linked retinal mutation, rd13. Mamm Genome 15:344–351.

Burgess DL, Kohrman DC, Galt J, Plummer NW, Jones JM, Spear B, Meisler MH (1995) Mutation of a new sodium channel gene, Scn8a, in the mouse mutant 'motor endplate disease.' Nat Genet 10:461–465.

Catterall WA, Goldin AL, Waxman SG (2005) International Union of Pharmacology. XLVII. Nomenclature and structure-function relationships of voltage-gated sodium channels. Pharmacol Rev 57:397–409.

Chen C, Bharucha V, Chen Y, Westenbroek RE, Brown A, Malhotra JD, Jones D, Avery C, Gillespie PJ 3rd, Kazen-Gillespie KA, Kazarinova-Noyes K, Shrager P, Saunders TL, Macdonald RL, Ransom BR, Scheuer T, Catterall WA, Isom LL (2002) Reduced sodium channel density, altered voltage dependence of inactivation, and increased susceptibility to seizures in mice lacking sodium channel beta 2-subunits. Proc Natl Acad Sci U S A 99:17072–17077.

Chen C, Westenbroek RE, Xu X, Edwards CA, Sorenson DR, Chen Y, McEwen DP, O'Malley HA, Bharucha V, Meadows LS, Knudsen GA, Vilaythong A, Noebels JL, Saunders TL, Scheuer T, Shrager P, Catterall WA, Isom LL (2004) Mice lacking sodium channel β1 subunits display defects in neuronal excitability, sodium channel expression, and nodal architecture. J Neurosci 24:4030–4042.

Chen Y, Yu FH, Sharp EM, Beacham D, Scheuer T, Catterall WA (2008) Functional properties and differential neuromodulation of Na(v)1.6 channels. Mol Cell Neurosci 38:607–615.

Cummins TR, Dib-Hajj SD, Herzog RI, Waxman SG (2005) $Na_v1.6$ channels generate resurgent sodium currents in spinal sensory neurons. FEBS Lett 579:2166–2170.

Cusdin FS, Clare JJ, Jackson AP (2008) Trafficking and cellular distribution of voltage-gated sodium channels. Traffic 9:17–26.

Dib-Hajj SD, Cummins TR, Black JA, Waxman SG (2007) From genes to pain: Na v 1.7 and human pain disorders. Trends Neurosci 30:555–563.

Dong C, Wu G (2006) Regulation of anterograde transport of alpha2-adrenergic receptors by the N termini at multiple intracellular compartments. J Biol Chem 281:38543–38554.

Drews VL, Lieberman AP, Meisler MH (2005) Multiple transcripts of sodium channel SCN8A (Na(V)1.6) with alternative 5′- and 3′-untranslated regions and initial characterization of the SCN8A promoter. Genomics 85:245–257.

Fujiwara T, Sugawara T, Mazaki-Miyazaki E, Takahashi Y, Fukushima K, Watanabe M, Hara K, Morikawa T, Yagi K, Yamakawa K, Inoue Y (2003) Mutations of sodium channel alpha subunit type 1 (SCN1A) in intractable childhood epilepsies with frequent generalized tonic-clonic seizures. Brain 126:531–546.

Fukuma G, Oguni H, Shirasaka Y, Watanabe K, Miyajima T, Yasumoto S, Ohfu M, Inoue T, Watanachai A, Kira R, Matsuo M, Muranaka H, Sofue F, Zhang B, Kaneko S, Mitsudome A, Hirose S (2004) Mutations of neuronal voltage-gated Na+ channel alpha 1 subunit gene SCN1A in core severe myoclonic epilepsy in infancy (SMEI) and in borderline SMEI (SMEB). Epilepsia 45:140–148.

George AL Jr (2005) Inherited disorders of voltage-gated sodium channels. J Clin Invest 115:1990–1999.

Harkin LA, McMahon JM, Iona X, Dibbens L, Pelekanos JT, Zuberi SM, Sadleir LG, Andermann E, Gill D, Farrell K, Connolly M, Stanley T, Harbord M, Andermann F, Wang J, Batish SD, Jones JG, Seltzer WK, Gardner A, Sutherland G, Berkovic SF, Mulley JC, Scheffer IE (2007) The spectrum of SCN1A-related infantile epileptic encephalopathies. Brain 130:843–852.

Herzog RI, Cummins TR, Ghassemi F, Dib-Hajj SD, Waxman SG (2003) Distinct repriming and closed-state inactivation kinetics of $Na_v1.6$ and $Na_v1.7$ sodium channels in mouse spinal sensory neurons. J Physiol 551:741–750.

Howell VM, de Haan G, Bergren S, Jones JM, Culiat CT, Michaud EJ, Frankel WN, Meisler MH (2008) A targeted deleterious allele of the splicing factor SCNM1 in the mouse. Genetics 180:1419–1427.

John VH, Main MJ, Powell AJ, Gladwell ZM, Hick C, Sidhu HS, Clare JJ, Tate S, Trezise DJ (2004) Heterologous expression and functional analysis of rat Nav1.8 (SNS) voltage-gated sodium channels in the dorsal root ganglion neuroblastoma cell line ND7–23. Neuropharmacology 46:425–438.

Kearney JA, Buchner DA, De Haan G, Adamska M, Levin SI, Furay AR, Albin RL, Jones JM, Montal M, Stevens MJ, Sprunger LK, Meisler MH (2002) Molecular and pathological effects of a modifier gene on deficiency of the sodium channel Scn8a (Na (v) 1.6). Hum Mol Genet 11:2765–2775.

Kearney JA, Wiste AK, Stephani U, Trudeau MM, Siegel A, Ramachandran-Nair R, Elterman RD, Muhle H, Reinsdorf J, Shields WD, Meisler MH, Escayg A (2006) Recurrent de novo mutations of SCN1A in severe myoclonic epilepsy of infancy. Pediatr Neurol 34:116–120.

Kile BT, Hentges KE, Clark AT, Nakamura H, Salinger AP, Liu B, Box N, Stockton DW, Johnson RL, Behringer RR, Bradley A, Justice MJ (2003) Functional genetic analysis of mouse chromosome 11. Nature 425:81–86.

Levin SI, Meisler MH (2004) Floxed allele for conditional inactivation of the voltage-gated sodium channel Scn8a (NaV1.6). Genesis 39:234–239.

Levin SI, Khaliq ZM, Aman TK, Grieco TM, Kearney JA, Raman IM, Meisler MH (2006) Impaired motor function in mice with cell-specific knockout of sodium channel Scn8a (NaV1.6) in cerebellar purkinje neurons and granule cells. J Neurophysiol 96:785–793.

Lopez-Santiago LF, Pertin M, Morisod X, Chen C, Hong S, Wiley J, Decosterd I, Isom LL (2006) Sodium channel beta2 subunits regulate

tetrodotoxin-sensitive sodium channels in small dorsal root ganglion neurons and modulate the response to pain. J Neurosci 26:7984–7994.
Lossin C, Wang DW, Rhodes TH, Vanoye CG, George AL Jr (2002) Molecular basis of an inherited epilepsy. Neuron 34:877–884.
Meisler MH, Kearney JA (2005) Sodium channel mutations in epilepsy and other neurological disorders. J Clin Invest 115:2010–2017.
Meisler MH, Plummer NW, Burgess DL, Buchner DA, Sprunger LK (2004) Allelic mutations of the sodium channel SCN8A reveal multiple cellular and physiological functions. Genetica 122:37–45.
Nabbout R, Gennaro E, Dalla Bernardina B, Dulac O, Madia F, Bertini E, Capovilla G, Chiron C, Cristofori G, Elia M, Fontana E, Gaggero R, Granata T, Guerrini R, Loi M, La Selva L, Lispi ML, Matricardi A, Romeo A, Tzolas V, et al. (2003) Spectrum of SCN1A mutations in severe myoclonic epilepsy of infancy. Neurology 60:1961–1967.
Okuse K, Malik-Hall M, Baker MD, Poon WY, Kong H, Chao MV, Wood JN (2002) Annexin II light chain regulates sensory neuron-specific sodium channel expression. Nature 417:653–656.
Osorio N, Alcaraz G, Padilla F, Couraud F, Delmas P, Crest M (2005) Differential targeting and functional specialization of sodium channels in cultured cerebellar granule cells. J Physiol 569:801–816.
Pfahnl AE, Viswanathan PC, Weiss R, Shang LL, Sanyal S, Shusterman V, Kornblit C, London B, Dudley SC Jr (2007) A sodium channel pore mutation causing Brugada syndrome. Heart Rhythm 4:46–53.
Poelzing S, Forleo C, Samodell M, Dudash L, Sorrentino S, Anaclerio M, Troccoli R, Iacoviello M, Romito R, Guida P, Chahine M, Pitzalis M, Deschênes I (2006) SCN5A polymorphism restores trafficking of a Brugada syndrome mutation on a separate gene. Circulation 114:368–376.
Poon WY, Malik-Hall M, Wood JN, Okuse K (2004) Identification of binding domains in the sodium channel Na(V)1.8 intracellular N-terminal region and annexin II light chain p11. FEBS Lett 558:114–118.
Raman IM, Sprunger LK, Meisler MH, Bean BP (1997) Altered subthreshold sodium currents and disrupted firing patterns in Purkinje neurons of Scn8a mutant mice. Neuron 19:881–891.
Rusconi R, Scalmani P, Cassulini RR, Giunti G, Gambardella A, Franceschetti S, Annesi G, Wanke E, Mantegazza M (2007) Modulatory proteins can rescue a trafficking defective epileptogenic Nav1.1 Na+ channel mutant. J Neurosci 27:11037–11046.
Rush AM, Dib-Hajj SD, Waxman SG (2005) Electrophysiological properties of two axonal sodium channels, Na_v1.2 and Na_v1.6, expressed in mouse spinal sensory neurones. J Physiol 564:803–815.
Schmidt JW, Catterall WA (1987) Palmitylation, sulfation, and glycosylation of the alpha subunit of the sodium channel. Role of post-translational modifications in channel assembly. J Biol Chem 262:13713–13723.
Spampanato J, Kearney JA, de Haan G, McEwen DP, Escayg A, Aradi I, MacDonald BT, Levin SI, Soltesz I, Benna P, Montalenti E, Isom LL, Goldin AL, Meisler MH (2004) A novel epilepsy mutation in the sodium channel SCN1A identifies a cytoplasmic domain for beta subunit interaction. J Neurosci 24:10022–10034.
Stockklausner C, Klocker N (2003) Surface expression of inward rectifier potassium channels is controlled by selective Golgi export. J Biol Chem 278:17000–17005.
Tan BH, Valdivia CR, Song C, Makielski JC (2006) Partial expression defect for the SCN5A missense mutation G1406R depends on splice variant background Q1077 and rescue by mexiletine. Am J Physiol Heart Circ Physiol 291:H1822–H1828.
Trudeau MM, Dalton JC, Day JW, Ranum LP, Meisler MH (2006) Heterozygosity for a protein truncation mutation of sodium channel SCN8A in a patient with cerebellar atrophy, ataxia, and mental retardation. J Med Genet 43:527–530.
Ulloa-Aguirre A, Janovick JA, Brothers SP, Conn PM (2004) Pharmacologic rescue of conformationally-defective proteins: implications for the treatment of human disease. Traffic 5:821–837.
Valdivia CR, Tester DJ, Rok BA, Porter CB, Munger TM, Jahangir A, Makielski JC, Ackerman MJ (2004) A trafficking defective, Brugada syndrome-causing SCN5A mutation rescued by drugs. Cardiovasc Res 62:53–62.
Van Wart A, Matthews G (2006) Expression of sodium channels Nav1.2 and Na_v1.6 during postnatal development of the retina. Neurosci Lett 403:315–317.
Waechter CJ, Schmidt JW, Catterall WA (1983) Glycosylation is required for maintenance of functional sodium channels in neuroblastoma cells. J Biol Chem 258:5117–5123.
West JW, Scheuer T, Maechler L, Catterall WA (1992) Efficient expression of rat brain type IIA Na+ channel alpha subunits in a somatic cell line. Neuron 8:59–70.
Wittmack EK, Rush AM, Craner MJ, Goldfarb M, Waxman SG, Dib-Hajj SD (2004) Fibroblast growth factor homologous factor 2B: association with Na_v1.6 and selective colocalization at nodes of Ranvier of dorsal root axons. J Neurosci 24:6765–6775.
Wittmack EK, Rush AM, Hudmon A, Waxman SG, Dib-Hajj SD (2005) Voltage-gated sodium channel Na_v1.6 is modulated by p38 mitogen-activated protein kinase. J Neurosci 25:6621–6630.
Wood JN, Bevan SJ, Coote PR, Dunn PM, Harmar A, Hogan P, Latchman DS, Morrison C, Rougon G, Theveniau M, Wheatley S (1990) Novel cell lines display properties of nociceptive sensory neurons. Proc Biol Sci 241:187–194.
Zhao J, Ziane R, Chatelier A, O'leary ME, Chahine M (2007) Lidocaine promotes the trafficking and functional expression of Na(v)1.8 sodium channels in mammalian cells. J Neurophysiol 98:467–477.
Zhou X, Dong XW, Crona J, Maguire M, Priestley T (2003) Vinpocetine is a potent blocker of rat NaV1.8 tetrodotoxin-resistant sodium channels. J Pharmacol Exp Ther 306:498–504.